# Pathway of membrane fusion with two tension-dependent energy barriers – EPAPS Appendices

Andrea Grafmüller, Julian Shillcock, and Reinhard Lipowsky
*Max Planck Institute of Colloids and Interfaces, Science Park Golm, 14424 Potsdam, Germany**
(Dated: May 1, 2007)

PACS numbers: 87.16.Dg, 61.20.Ja, 82.70.-y
Keywords:

### App. A. DPD method and parametrization

In our DPD simulations, we studied the same systems as in [1, 2] but for a different set of parameters. In order to make our presentation self-contained, we start with a brief review of the DPD method and parametrization [3–7].

The DPD model is built up from soft particles or beads that represent several atoms or molecules. The beads are distinguished by the label $i = 1, 2, \ldots, N_b$, where $N_b$ denotes the total number of beads, and can represent different particle species as described by $s_i$. The systems considered here are built up from three such species, lipid head (H), lipid chain (C), and water (W) beads, and the variable $s_i$ can thus attain the three values H, C, and W. The lipid molecules have a headgroup consisting of three H beads and two chains, each of which consists of four C beads. The latter architecture was introduced in the context of molecular dynamics simulations [8] and also used in our previous DPD simulations [1, 2].

As explained in [8], each C bead represents 3.5 $CH_2$ groups which implies that one chain with four beads corresponds to a chain length of 14 such groups. Therefore, the molecular architecture considered here provides a coarse-grained model for the phospholipid DMPC that has two chains, each of which consists of 14 $CH_2$ groups. Furthermore, we choose (i) our basic length scale to match the experimentally observed membrane area per DMPC molecule as given by 0.596 $nm^2$ [9] and (ii) our basic time scale to match the experimentally observed diffusion constant, $D \simeq 5\ \mu m^2/s$ [10], for lateral diffusion of DMPC within the bilayer membrane.

Two beads $i$ and $j$ experience three types of forces: (i) A conservative force $\mathbf{F}_{ij}^C$, which represents a coarse-grained description of the intermolecular interactions between the atoms or molecules contained in the beads; (ii) A random force $\mathbf{F}_{ij}^R$, which represents thermal noise; and (iii) A dissipative force $\mathbf{F}_{ij}^D$, which must be added in order to ensure the dissipation-fluctuation theorem in equilibrium [4]. Together, the random and the dissipative force provide the thermostat of the system. This thermostat is constructed in such a way that it conserves particle or bead momentum [3].

The beads are taken to be spherical, and their centers have position vectors $\mathbf{r}_i$ and velocities $\mathbf{v}_i$. For two beads $i$ and $j$, the conservative interparticle force, $\mathbf{F}_{ij}^C$, depends on the interparticle distance $r_{ij} \equiv |\mathbf{r}_i - \mathbf{r}_j|$ and the unit vector $\hat{\mathbf{r}}_{ij} \equiv (\mathbf{r}_i - \mathbf{r}_j)/r_{ij}$ pointing from $j$ to $i$. This force is taken to be softly repulsive and given by

$$\begin{aligned} \mathbf{F}_{ij}^C &\equiv a_{ij}(1 - r_{ij}/r_o)\,\hat{\mathbf{r}}_{ij} \qquad \text{for} \quad r_{ij} \le r_0 \\ &\equiv 0 \qquad\qquad\qquad\qquad\ \ \text{for} \quad r_{ij} > r_0\ . \end{aligned} \tag{1}$$

which involves only two parameters: (i) the force amplitude $a_{ij} > 0$, which depends on the species of the two beads, i.e., $a_{ij} = a(s_i, s_j)$, and (ii) the force range $r_o$, which is taken to be independent of the bead pair $(i, j)$.

The dissipative force between two beads $i$ and $j$ is linear in their relative velocity $\mathbf{v}_{ij} = \mathbf{v}_i - \mathbf{v}_j$ (which is proportional to their relative momentum since all beads have the same mass) and takes the form

$$\mathbf{F}_{ij}^D = -\gamma_{ij}(1 - r_{ij}/r_o)^2(\hat{\mathbf{r}}_{ij}.\mathbf{v}_{ij})\,\hat{\mathbf{r}}_{ij}, \tag{2}$$

with friction coefficients $\gamma_{ij}$. Finally, the random force $\mathbf{F}_{ij}^R$ acting between beads $i$ and $j$ is parametrized as

$$\mathbf{F}_{ij}^R = \sqrt{2\gamma_{ij}k_BT}(1 - r_{ij}/r_o)\,\zeta_{ij}\,\hat{\mathbf{r}}_{ij}, \tag{3}$$

with thermal energy $k_BT$ and random variables $\zeta_{ij}$. The latter variables are distributed symmetrically and uniformly with $\langle\zeta_{ij}(t)\rangle = 0$ and $\langle\zeta_{ij}(t)\zeta_{i'j'}(t')\rangle = (\delta_{ii'}\delta_{jj'} + \delta_{ij'}\delta_{ji'})\delta(t-t')$, and fulfill the symmetry property $\zeta_{ij}(t) = \zeta_{ji}(t)$.

The H and C beads of a lipid molecule are connected by harmonic spring potentials $U_2 = (1/2)k_2(r_{i,i+1} - l_0)^2$ which are parametrized by the spring constant $k_2$ and the unstretched length $l_o$. The hydrocarbon chains are stiffened by the three-body potential $U_3 = k_3\,[1 - cos(\psi - \psi_o)]$ which depends on the bending stiffness $k_3$, the tilt angle $\psi$ between two consecutive bonds, and the prefered tilt angle $\psi_o$. This parameterization was introduced in the context of molecular dynamics simulations [8] and also used in our previous DPD simulations [1, 2].

In the DPD simulations reported here, we used the following parameter set. The values of the spring constant $k_2$ and the unstretched length $l_0$ were taken to be $k_2 = 128k_BT/r_o^2$ and $l_o = 0.5\,r_o$ as in our previous fusion simulations [2]. The tail chains of the lipid molecules had the bending stiffness $k_3 = 15$, which is somewhat smaller than the value $k_3 = 20$ used in [2], and the prefered tilt angle $\psi_o = 0$ as in [2]. The friction coefficients $\gamma_{ij}$ had the same values as in [1, 2] but the force amplitudes $a_{ij}$ were chosen differently.

As previously mentioned, the force amplitudes depend on the species of the two beads, i.e., $a_{ij} = a(s_i, s_j)$ with

(a)

| $a_{ij}$ | H | C | W |
|---|---|---|---|
| H | 25 | 50 | 35 |
| C | 50 | 25 | 75 |
| W | 35 | 75 | 25 |

(b)

| $a_{ij}$ | H | C | W |
|---|---|---|---|
| H | 30 | 35 | 30 |
| C | 35 | 10 | 75 |
| W | 30 | 75 | 25 |

TABLE I: DPD parameters $a_{ij}$ which represent the amplitudes of the repulsive DPD forces between two beads $i$ and $j$. These forces depend on the species $s_i$ and $s_j$ of the two beads, i.e., $a_{ij} = a(s_i, s_j)$ where $s_i$ and $s_j$ can attain the three values H (lipid head), C (lipid chain), or W (water). (a) Old parameter set used in [2]; and (b) New parameter set used in the present study. The two parameter sets lead to bilayer membranes that differ (i) in their stretching behavior, see Fig. 1, and (ii) in their stability with respect to intermembrane flipflops.

$s_i$ = H, C, or W. A typical set of force amplitudes as used in our previous DPD simulations [1, 2] is shown in Table I(a). The new set of force amplitudes $a_{ij}$ as used here is displayed in Table I(b). Comparison of these two tables shows that all amplitudes $a_{ij}$ have been changed apart from those between two W beads and between a C and a W bead. Note that all $a_{ij}$ values displayed in Table I satisfy $a_{ij} \geq 10$, which ensures correct diffusive behavior of the beads as discussed in [7].

Both the new and the old set of parameters lead to fluid bilayers that arise from the spontaneous self-assembly of the lipid molecules, and exhibit tensionless bilayer states without interdigitation between the lipid chains in the two monolayers. In addition, for both parameter sets, the tensionless state of the planar membrane is characterized by the dimensionless molecular area $A/Nr_o^2 \simeq 1.25$. However, the membranes obtained from the two parameter sets, show qualitative differences (i) in their overall stretching behavior, see App. B below, and (ii) in the stability of two adhering membranes with respect to flips of lipid molecules between these membranes. Whereas the new parameter set leads to an energy barrier of about $10\,k_BT$ for these intermembrane flips as described in the main text, no such barrier could be detected for the old parameter set.

This difference in behavior can be understood in a simple way if one considers the ratio $a_{\rm HC}/a_{\rm CC}$ which gives the strength of the repulsion between one H and one C chain bead relative to the one between two C beads. For the old parameter set in Table I(a), one has $a_{\rm HC}/a_{\rm CC} = 2$ whereas the new parameter set in Table I(b) leads to the increased ratio $a_{\rm HC}/a_{\rm CC} = 3.5$, which implies an enhanced repulsive interaction between the H and C beads.

### App. B. Tension as a function of molecular area

In contrast to the value of the molecular area in the tensionless state, the stretching behavior of the membranes is rather different for the two parameter sets. For the old parameter set, the dimensionless tension $\bar{\Sigma} \equiv \Sigma r_0^2/k_BT$ is a nonlinear function of the dimensionless molecular area $\bar{A} = A/Nr_o^2$ as shown in Fig. 1, and this area can be increased from $\bar{A} \simeq 1.25$ to $\bar{A} \simeq 2.05$, i.e., by about 60 percent, without rupturing the membrane within a few $\mu$s. Experimental studies of large vesicles, on the other hand, yield a maximal extensibility of 3 to 5 percent [11] for lipid bilayers and of about 20 percent for polymersomes [12]. The new parameter set in Table I(b) reduces the bilayer's stretchability to about 20 percent and leads to an essentially linear relationship between tension $\bar{\Sigma}$ and molecular area $\bar{A}$, see Fig. 1.

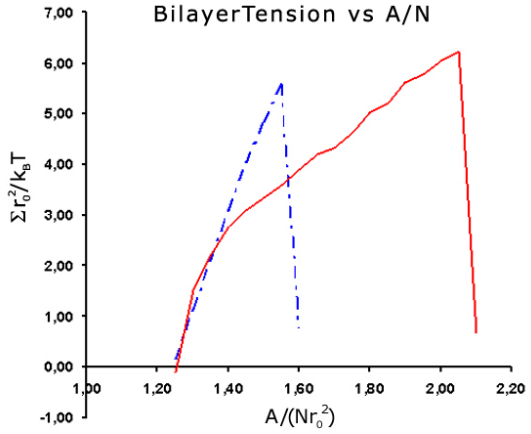


FIG. 1: Bilayer tension versus area per molecule. Red: standart dpd parameters, Blue: New parameter set, with improved stretching behavior. Solid: standart parameter set used in the described fusion events, dashed: with $a_{HT}$ parameter increased to 50, dashed-dotted: same as solid in the larger boxsize $((72r_0)^3$ used for the fusion protocol

The area compressibility modulus $K_A$ is proportional to the slope of the tension as a function of molecular area. The corresponding dimensionless modulus $\bar{K}_A = K_A r_0^2/k_BT$ can be read off from Fig. 1 and is found to be $\bar{K}_A = 18.2$.

### App. C. Frequencies of different pathways

Our fusion protocol starts from a vesicle preassembled close to a planar membrane spanning the simulation box. The vesicle is assembled within a spherical shell of outer radius $R_{\rm ex} = 7.5$ or 15 nm. The inner radius $R_{\rm in}$ is equal to the outer radius minus the thickness of the planar membrane. Within this spherical shell, we accommodate two monolayers of lipid molecules that are arranged as equally spaced as possible. On the outer surface of the spherical shell, we place $N_{\rm ex} = 4\pi R_{\rm ex}^2/A_{\rm ve}$ lipid head groups where $A_{\rm ve}$ is the prescribed molecular area of a lipid within the vesicle membrane. Likewise, on the inner surface of the shell, we place $N_{\rm in} = 4\pi R_{\rm in}^2/A_{\rm ve}$ such head groups. The chains of all of these molecules are taken to point initially towards or away from the center of the

| | 1.10 | | | | 1.15 | | | | 1.20 | | | |
|---|---|---|---|---|---|---|---|---|---|---|---|---|
| 1.35 | | | | | A | HF | F | R | A | HF | F | R |
| | | | | | 0 | 4 | 2 | 0 | 0 | 4 | 2 | 0 |
| 1.40 | A | HF | F | R | A | HF | F | R | A | HF | F | R |
| | 1 | 0 | 5 | 0 | 3 | 0 | 3 | 0 | 1 | 2 | 3 | 0 |
| 1.45 | A | HF | F | R | A | HF | F | R | A | HF | F | R |
| | 0 | 1 | 5 | 0 | 0 | 1 | 5 | 0 | 0 | 0 | 6 | 0 |
| 1.50 | A | HF | F | R | A | HF | F | R | A | HF | F | R |
| | 0 | 0 | 5 | 1 | 0 | 0 | 5 | 1 | 0 | 0 | 6 | 0 |
| 1.55 | A | HF | F | R | A | HF | F | R | A | HF | F | R |
| | 0 | 0 | 1 | 4 | 0 | 0 | 3 | 3 | 0 | 0 | 4 | 2 |

TABLE II: Observed frequencies of different pathways for 83 simulation runs of a 15 nm vesicle in contact with a planar membrane. The first row and first column contain the initial molecular areas $\bar{A}_{\rm ve}$ and $\bar{A}$ of the vesicle and planar membrane, respectively. The different pathways are adhesion (A), hemifusion (HF), fusion (F), and rupture (R).

| | 1.10 | | | | 1.15 | | | | 1.20 | | | |
|---|---|---|---|---|---|---|---|---|---|---|---|---|
| 1.45 | A | HF | F | R | A | HF | F | R | A | HF | F | R |
| | 4 | 0 | 1 | 0 | 2 | 0 | 4 | 0 | 1 | 2 | 3 | 0 |
| 1.50 | A | HF | F | R | A | HF | F | R | A | HF | F | R |
| | 1 | 1 | 4 | 0 | 0 | 1 | 4 | 1 | 0 | 1 | 10 | 0 |
| 1.55 | A | HF | F | R | A | HF | F | R | A | HF | F | R |
| | 0 | 0 | 4 | 2 | 0 | 0 | 5 | 1 | 0 | 1 | 5 | 3 |

TABLE III: Observed frequency of different pathways for 61 simulation runs of a 30 nm vesicle in contact with a planar membrane. The notation is the same as in Table II.

shell.

Both vesicle and planar membrane consist of the same type of lipid molecules with interactions as described in App. A. The membranes are put under tension by varying the number of lipid molecules at constant box area or vesicle radius. Two systems with different vesicle diameters of 15nm and 30nm were simulated. The box area, which is equal to the projected area of the blanar membrane, was $(50\,\mathrm{nm})^2$ in both cases while the box height was 35 and 50 nm for the 15 and 30 nm vesicle, respectively.

For all simulation runs, the two membranes attained one out of four possible states after about 12 $\mu$s which represents the maximal time scale accessible to the simulations: the membranes form an adhering (A), hemifused (HF), or fused (F) state unless one of them ruptured (R), see Table II and Table III.

One should note that successful fusion events were always observed to proceed, on intermediate time scales, via adhering and hemifused states. Thus, the adhering and hemifused states that we observed after about 12 $\mu$s as displayed in Table II and Table III might still fuse if we extended the simulations to longer time scales.


* `www.mpikg.mpg.de/theory/`

[1] J. C. Shillcock and R. Lipowsky. *J. Chem. Phys.* **117**, 5048 (2002).

[2] J. Shillcock and R. Lipowsky. *Nature Materials* **4**, 225 (2005).

[3] P.J. Hoogebrugge and J.M.V.A. Koelman. *Europhys. Lett.* **19**, 155 (1992).

[4] P. Español and P. Warren, *Europhys. Lett.* **30**, 191 (1995).

[5] R.D. Groot and P.B. Warren. *J. Chem. Phys.* **107**, 4423 (1997).

[6] I. Vattulainen, M. Karttunen, G. Besold, and J.M. Polson. *J. Chem. Phys.* **116**, 3967 (2002).

[7] S. D. Stoyanov and R. D. Groot. *J. Chem. Phys.* **122**, 114112 (2004).

[8] R. Goetz and R. Lipowsky. *J. Chem. Phys.* **108**, 7397 (1998); and R. Goetz, G. Gompper, and R. Lipowsky. *Phys. Rev. Lett.* **82**, 221 (1999).

[9] J. Nagle and S. Tristram-Nagle, Biochim. Biophys. Acta **1469**, 159 (2000).

[10] G. Orädd, G. Lindblom, and P. W. Westerman, Biophys. J. **83**, 2702 (2002).

[11] E. Evans and W. Rawicz. *Phys. Rev. Lett.* **64**, 2094 (1990).

[12] B.M. Discher, Y.-Y. Won, D.S. Ege, J. C.-M. Lee, F.S. Bates, D.E. Discher, and D.A. Hammer. *Science* **284**, 1143 (1999).